Journal of Power Sources 230 (2013) 194–200

Contents lists available at SciVerse ScienceDirect

Journal of Power Sources

journal homepage: www.elsevier.com/locate/jpowsour

Performance measurements of a single cell flowing electrolyte-direct methanol fuel cell (FE-DMFC)

Nasim Sabet-Sharghi [a,*], Cynthia Ann Cruickshank [a], Edgar Matida [a], Feridun Hamdullahpur [b]

[a] Mechanical and Aerospace Eng. Department, Carleton University, Ottawa, ON, Canada K1S 5B6
[b] Mechanical Engineering Department, University of Waterloo, Canada

HIGHLIGHTS

- Demonstrating a unique design for the flowing electrolyte-direct methanol fuel cell.
- Demonstrating that flowing electrolyte can remove methanol.
- 3 M sulphuric acid was identified as the preferred flowing electrolyte concentration.
- The effects of the flowing electrolyte on the overall performance were studied.

ARTICLE INFO

Article history:
Received 17 August 2012
Received in revised form
1 November 2012
Accepted 26 November 2012
Available online 21 December 2012

Keywords:
Flowing electrolyte
Direct methanol fuel cell
Methanol crossover
Nafion

ABSTRACT

The performance of a single cell flowing electrolyte-direct methanol fuel cell (FE-DMFC) was experimentally studied and its performance was compared to a regular DMFC. The active area of the fuel cell was approximately 25 cm^2. Serpentine channels were used for both the methanol and air flows. Two combinations of Nafion® polymer electrolyte membranes (PEMs) were used in the MEAs. These were NR-212/N-117 (Type 1) and NR-212/NR-212 (Type 2). For this study, diluted sulphuric acid was used as the electrolyte, which flows through a channel made of a polyethylene porous material. The flowing electrolyte conditions (e.g., flow rate, channel thickness and sulphuric acid concentration), the methanol concentration, and the fuel cell temperatures were varied to study how these parameters affect the overall performance of the FE-DMFC. Type 1 MEA used in conjunction with 2 M methanol produced the highest current density. The power density decreased when the thickness of the flowing electrolyte channel was increased, and the performance of the fuel cell increased when the temperature of the fuel cell was increased, as expected. The results show that the performance of the present FE-DMFC was similar to a DMFC using the same active area and a single MEA (Nafion® N-117).

1. Introduction

Direct methanol fuel cells (DMFCs) are a subset of polymer electrolyte membrane fuel cells, which use proton exchange membranes as the electrolyte and diluted methanol as fuel. Direct methanol fuel cells are primarily targeted towards small scale technologies (normally smaller than 1 kW) and relatively low operating temperatures in the range of 60–90 °C [1]. This type of fuel cell is becoming more attractive when size and weight are important, as in the case of portable devices used in military operations, as well as, in other civilian applications (e.g., laptop computers, cellular phones, toys). Methanol is also easy to transport and store, requiring infrastructure similar to gasoline, which is currently available. These types of fuel cells are also competitive against current lithium-ion rechargeable batteries when power density is concerned [2,3].

There are a number of issues which exist, however, that reduce the performance of DMFCs. These include slow reaction kinetics of methanol due to the multi-step fuel oxidation process affecting anodic overpotentials [4], and the catalyst poisoning due to the intermediate hydrocarbon species produced during methanol oxidation. The most significant issue, however, related to DMFCs is the crossover of methanol from the anode to the cathode through the PEM. This latter issue significantly reduces the overall performance of the DMFC [5–9]. This study addresses the methanol crossover issue.

The concept of a direct methanol fuel cell with a flowing electrolyte was introduced by Kordesch et al. in 2001 [10]. In this

* Corresponding author. Tel.: +1 972 54 241 4127; fax: +1 972 4 831 3344.
E-mail address: nasim84@gmail.com (N. Sabet-Sharghi).

0378-7753/$ – see front matter © 2012 Elsevier B.V. All rights reserved.
http://dx.doi.org/10.1016/j.jpowsour.2012.11.147

design, the electrolyte diffuses through a porous spacer located between the two electrodes and removes any crossed over methanol from the cell before it reaches the cathode. A schematic of a single flowing electrolyte-direct methanol fuel cell (FE-DMFC) is shown in Fig. 1. Other advantages of FE-DMFCs include simple water and heat management and the possibility of removing reaction by-products such as aldehyde residues and carboxylic acids. It should be noted, however, that the system is more complex due to various added components [11].

Over the past decade, limited work has been conducted on FE-DMFCs. Jayashree et al. [12,13] explored the concept proposed by Choban et al. [14] and tested the liquid electrolyte concept in a membraneless microfluidic hydrogen fuel cell, where they used diluted methanol as the fuel and dissolved oxygen in sulphuric acid. In this design, the two liquid streams and the liquid–liquid interface provided the ionic conductance of the fuel cell [14]. Hollinger et al. tested the same concept on a micro scale laminar flow fuel cell [15]. They performed their experiments with 1 M sulphuric acid, 1 M methanol and pure oxygen at 80°°C. The fuel cell's highest performance was obtained using a nanoporous material. This combination gave them a maximum open circuit voltage (OCV) of 0.64 V and power density of 70 mW cm^{-2} [15].

As shown in Fig. 1, in a FE-DMFC, the fuel enters the cell through the anode inlet and diffuses through the porous anode. After the oxidisation reaction at the catalyst layer, any unreacted fuel along with products will exit from the outlet. The protons will go through the PEM while the electrons will be conducted through an electrical connection from the anode to the cathode and through an external load. The fluid electrolyte will remove any unreacted fuel or products that pass through the PEM along with the protons; however, being acidic, the electrolyte will let the protons cross to the cathode side. The oxidant is provided to the cathode through the inlet and after the reduction reaction, the products are expelled through the outlet [16].

One of the shortcomings of FE-DMFC is the management of the flowing electrolyte itself. The flowing electrolyte circulation system can be divided into four categories: 1) non-circulating flowing electrolyte: fresh electrolyte is used and the contaminated electrolyte is stored in a container; the used electrolyte will be retrieved and recycled in separate industrial facilities, 2) circulating flowing electrolyte: this method circulates the electrolyte repeatedly and requires electrolyte change from time to time, 3) circulating electrolyte with in-situ purification: in this method, the methanol is separated from the electrolyte in the device; this method is not viable due to compactness reasons, and 4) circulating electrolyte going through an additional DMFC: in this method, the electrolyte waste goes through a DMFC in order for the methanol inside the electrolyte to be consumed. It should be noted that the flowing electrolyte management system was not a focus of this work. In the present work, the performance of single cell FE-DMFC using two different MEAs are tested experimentally and compared against a single cell DMFC.

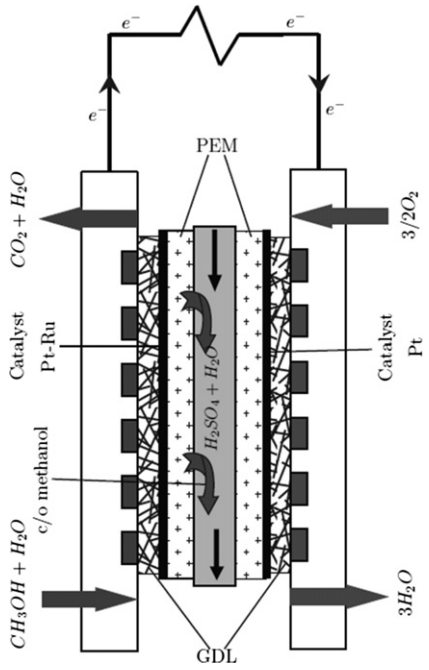

Fig. 1. Schematic of a FE-DMFC.

2. Methods

2.1. FE-DMFC design

Fig. 2 illustrates a three dimensional model of the FE-DMFC used in the present study. Special care was taken to select materials that are resistant to sulphuric acid and several configurations were tested to resolve leakage issues.

The end plates (Item 1 in Fig. 2) are made of stainless steel (13 mm thick) to protect the structure of the fuel cell while providing an even compression distribution on the inner components of the cell. Heating pads were also attached to these plates. Polytetrafluoroethylene (PTFE) sheets (Item 2) were used to electrically insulate the end plates from the current collectors (Item 3), which consisted of copper plates (1.25 mm thick) with 1 micron gold plating.

Grade AR-08 graphite was used for the reactant distributor plates (Item 4). Parallel serpentine channels were machined over the surface of the plates (a serpentine channel area of 25 cm^2) providing the methanol and air passages in the fuel cell. Fig. 3 shows a 3-D model of the graphite plates used in this study. The plate on the right has six openings that allow the flow management of methanol, air and electrolyte. Air flows in this plate from top to bottom as the labels Airin and Airout indicate. The electrolyte enters the plate from the top and flows in the cell through a porous channel (Item 9 in Fig. 2) and exits at the bottom. The terms Min and Mout (indicated on the left plate) are the inlet and outlet of the diluted methanol, respectively. The diluted methanol flows from the bottom of the channel to the top of the plate in order to promote CO_2 removal from the system. The air, flowing electrolyte

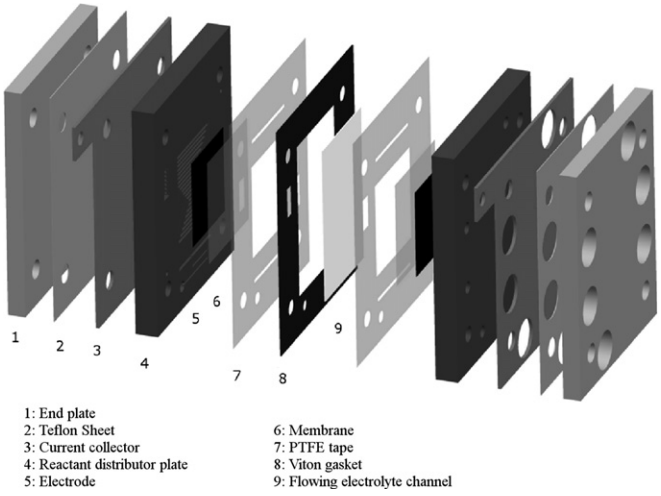

Fig. 2. FE-DMFC assembly.

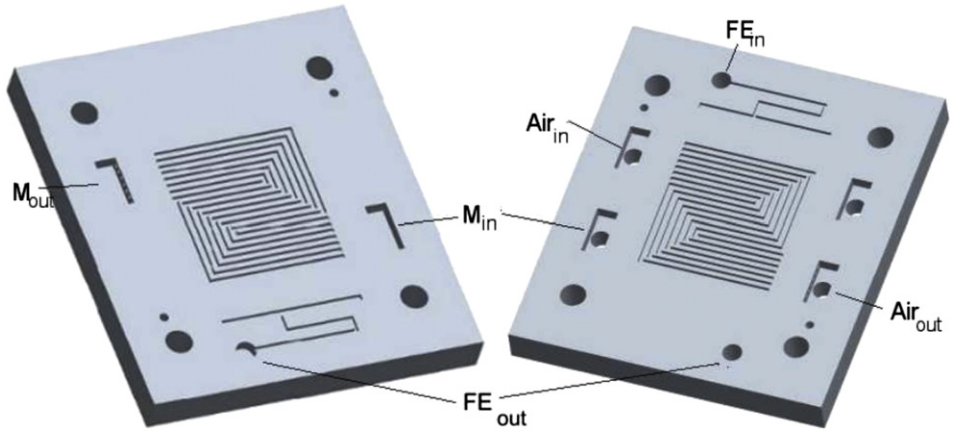

Fig. 3. A 3-D model of the graphite plates used in this study.

and methanol flows are separated and sealed by membranes and gaskets following the design shown in Fig. 2.

The anode and cathode consist of a gas diffusion layer (GDL) and a catalytic layer, both shown as Item 5 in Fig. 2. For this study, commercially available anode and cathode electrodes from Alfa Aesar® were used. Specifically, the gas diffusion layer and catalyst consisted of Toray carbon paper (TGP-H-090) along with 2 mg cm^{-2} Pt on the cathode and 2.7 mg cm^{-2} Pt on the anode. The anode also had 1.35 mg cm^{-2} Ru. The percent composition list of the electrodes is shown in Table 1.

Another important component of the fuel cell is the membrane (Item 6 in Fig. 2). Polymer exchange membranes are the most commonly used electrolytes in DMFCs. In this study, the PEM used was Nafion®. Nafion® sheets are produced in 1100 and 2100 g equivalent weight membranes. For this work, Nafion® N-117 and Nafion® NR-212 were used and measure 7 and 2 mil thick, respectively (where 1 mil is one thousandth of an inch).

Gaskets are used to seal the fuel cell and provide proper thickness for the flowing electrolyte channel. In this case, it was necessary to find a gasket that was resistant to sulphuric acid at elevated temperature. After considerable testing with several materials and designs, PTFE tape and Viton® (fluoroelastomer) sheets were selected to perform the current study. Wide PTFE tape that covered the whole graphite plate was used to fasten the MEA over the serpentine channel. The tape used was 89 μm thick and the dielectric strength was up to 9000 V. The gasket consisted of numerous layers of Viton® sheets, since they have adequate heat and chemical resistance.

The flowing electrolyte channel should also serve as a back pressure provider for the Nafion® in order to prevent the Nafion® sheets from coming in contact. A hydrophilic porous polyethylene sheet was tested and chosen as the flowing electrolyte channel. POREX and Vyon were identified as the hydrophilic polyethylene material to be tested in this study. Using a rigid material next to Nafion® ensured that the two Nafion® sheets would not come into contact and also the swelling of the Nafion® would be limited. The microporous and hydrophilic properties of these materials ensure the transfer of ions. Polyethylene is also resistant to sulphuric acid. Table 2 shows the specifications for these materials. Channel thicknesses of 0.6, 1.5, and 2 mm were tested.

Table 1
Percent composition list of electrodes.

Components	%
Non-woven carbon fibre	60
Catalyst	25
Carbon black	5
Polytetrafluoroethylene (PTFE)	5
Polyfluorosulphonicacid (PFSA) ionomer	5

2.2. Fabrication and assembly

The Nafion® had to be cleaned, activated and hydrated before it could be used in the fuel cell. Based on the procedure adapted by Kordesch [16] Nafion® membranes were kept in a warm solution (80–100°C) of 3% hydrogen peroxide, distilled water, 0.5 M sulphuric acid and distilled water again for 1 h at each solution. Hydrogen peroxide (H_2O_2) was used to remove organic contaminants from the surface of the membrane [5], distilled water was used for hydration, and sulphuric acid was used for activation and full protonation of the Nafion® [17,18]. The Nafion® sheets were then stored in distilled water until they were prepared for heat pressing.

Heat pressing allows good interfacial contact when assembling the membrane with the electrodes [19]. The Carver Laboratory Press (Model no: 2697-5) was used for heat pressing in this study. Based on the method explained by Zhang et al. [19], each of anode and cathode electrodes were heat pressed to a different membrane at a pressure and temperature of 3 MPa and 180°C, respectively, for 3 min. Although partial delamination sometimes occurred using these conditions, the majority of the GDL surface area stayed attached to the Nafion®.

All of the components discussed above were assembled and fastened by grade 8 bolts, which were electrically insulated using heat shrink tubing. Preliminary testing had shown that closing the fuel cell assembly with a 10.13 N m (90 in-lb) torque produced the best performance. Lower compression force resulted in leakages, while higher force would crush the electrodes. In a study conducted by Zhu et al., it was shown that the compression force has a significant effect on the ohmic and mass transfer resistances [20].

It was observed that hot pressing caused dehydration of the Nafion® membrane which resulted in low ionic conductivity [18,21]. Therefore, a conditioning operation was conducted after the MEAs

Table 2
Flowing electrolyte channel specifications.

Brand	Thickness [mm]	Pore size [μm]
POREX	0.61	75–110
POREX	1.5	50–90
Vyon	2.0	20–40

were installed in the fuel cell in order to increase the ionic conductivity of the membrane and also enhance the catalytic reactions [18]. Since the purpose of the rehydration process was to hydrate the membrane and improve the ionic conductivity of the membrane, the method used was based on the one developed by Tse [18]. This method involves pumping the water through the fuel and the flowing electrolyte channels while Nitrogen gas is supplied to the oxidant channels until the cell reaches 85°°C. In the next step, 2 M methanol, 2 M sulphuric acid and air are supplied to the fuel, flowing electrolyte and oxidant channel, respectively. The fuel cell is then operated at an open circuit voltage and 0.3 V for 15 min each, repeatedly for 8 h or until the current and voltage reach a stable state.

2.3. Experimental setup

Fig. 4 shows a schematic of the experimental setup. Diluted methanol and sulphuric acid were pumped to the cell by a tubing pump (MASTERFlex C/L Pump) and a DC pump (Fluid metering Inc., RHB), respectively. Digital pressure transducers (GE Druck PMP 1210) were installed to measure pressure prior to the fluids entering the cell. Needle valves were installed at the outlets of the cell, allowing pressure control. Air was supplied from a compressor and passed through an air filter and a manometer. The temperatures of the cell and the methanol inlet were measured by calibrated Type K thermocouples connected to an Omega temperature controller, which controlled the energy transfer to the heaters that were attached to the end plates by a relay.

A Fideris electronic load (Innovator Series-250 kW) was used in order to measure the output performance of the cell. For this study, all experiments were performed at a cell temperature of 85 °C.

Results from the uncertainty analysis include a bias error of 12 mV and 3.4 mA cm^{-2} for voltage and current density, respectively. The random error was also found to be 14 mV and 4.6 mA cm^{-2} for voltage and current density, respectively. For the maximum power density, where the current density is 136.3 mA cm^{-2} and voltage is 247.4 mV, the uncertainty analysis indicated that the 99% and 95% confidence levels were 18.5% and 14%, respectively.

3. Results and discussion

In this study, two different types of membrane electrode assemblies were constructed. Table 3 contains a list of components that make up these MEAs. The total Nafion® thickness for Type 1 and Type 2 MEAs was 9 (i.e., 7 + 2) and 4 (i.e., 2 + 2) mil, respectively. The thinner membranes were selected to reduce ohmic losses in the fuel cell. Fig. 5 illustrates the MEA types used in this study. It should be noted that the components are not drawn to scale.

Table 3
MEA structure.

Type 1	Cathode + Nafion® 117 + FE channel + Nafion® 212 + Anode
Type 2	Cathode + Nafion® 212 + FE channel + Nafion® 212 + Anode
DMFC	Cathode + Nafion® 117 + Anode

3.1. Effects of membrane thickness

The thickness and equivalent weight of the membrane is one of the most contributing factors that determine the amount of methanol crossover. Many researchers have concluded that the thicker membrane allows less methanol to crossover [11,15,19]. Table 4 shows the maximum power density generated by Type 1 and Type 2 MEAs for FE-DMFC with 0.6 FE channel, as well as, a regular DMFC operating with 0.5 M and 2 M methanol. The Type 1 MEA contained 117 and 212 Nafion® while the Type 2 had two sheets of Nafion® 212.

Figs. 6 and 7 show the performance of the fuel cell with different MEAs for 0.5 and 2 M methanol solution, respectively. It can be concluded from Fig. 6 and Table 4 that when comparing the two FE-DMFCs, the thinner MEA (Type 2 MEA) produced the highest power density for less concentrated methanol due to lower internal resistance. The maximum power density of 34.6 mW cm^{-2} was achieved at a current density of 132.4 mA cm^{-2}. Fig. 7 demonstrates that the thicker MEA performed best when a higher concentration of methanol was used since thicker PEM prevented more methanol crossover. In this case, the fuel cell generated a maximum power density of 33.7 mW cm^{-2} at a current density of 136.3 mA cm^{-2}.

The regular DMFC has a similar OCV to Type 1 MEA, which indicates that the methanol crossover levels were similar. The OCV of the Type 2 MEA, however, was lower than the other two due to more methanol crossing over at the initial stage. Therefore, it can be concluded that the thinner MEA allowed more methanol crossover

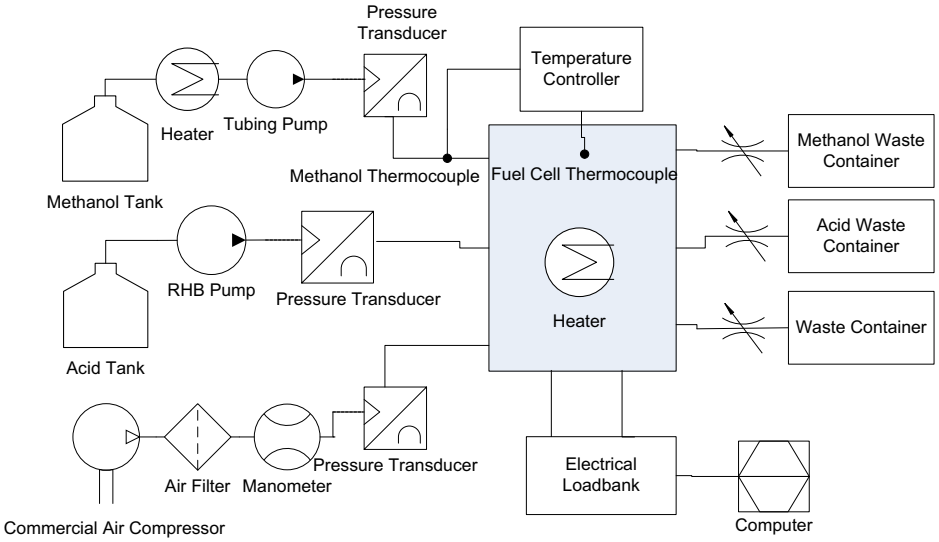

Fig. 4. Schematic of experimental setup.

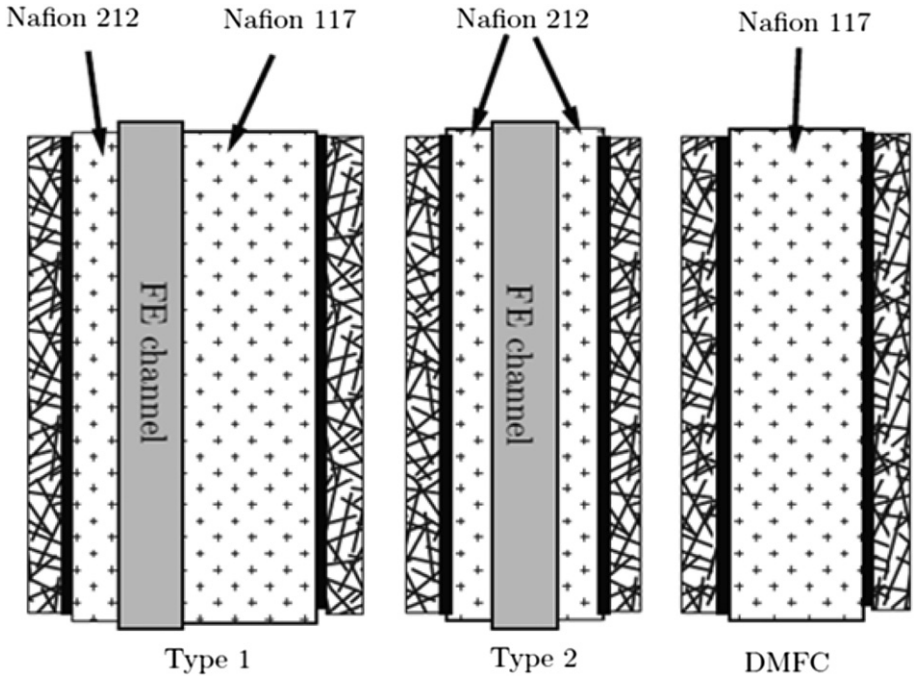

Fig. 5. MEA configurations.

while it had lower resistance and the thicker MEA generated a similar amount of power not only by facilitating less methanol crossover at higher initial concentration, but also contributed more to ohmic resistance. Comparing the two types of FE-DMFC membranes with a regular DMFC shows that the flowing electrolyte channel caused a higher internal resistance; hence lower resistance in the DMFC resulted in higher power generated by the fuel cell.

3.2. Effects of flowing electrolyte concentration

Electrolytes dissociate in polar solvents to form charged species (ions) [22]. Strong acids fully dissociate in water to produce H^+ or hydronium ions (H_3O^+) [23]. For strong electrolytes, the resistivity and the conductivity are dependent on the electrolyte concentration [22,23]. At higher concentrations, the conductivity is lower than direct proportionality, which is due to constricted ionic movement as a result of higher interionic forces [22]. Sulphuric acid is mostly conductive at approximately 35% by mass (which corresponds to 3 M) and the conductivity increases with temperature [24].

Fig. 8 illustrates the performance of the fuel cell for 1 M (10% by mass), 2 M (20% by mass) and 3 M (35% by mass) sulphuric acid and Table 5 summarises the maximum power and the corresponding current density generated by the fuel cell for each FE concentration. The slope of the polarisation curve is higher for the 1 M acid, which indicates higher ohmic resistance due to low proton conductivity. The maximum power density reached with 1 M sulphuric acid was 21.8 mW cm^{-2} at a current density of 79 mA cm^{-2}. Increasing the concentration of sulphuric acid to 2 M increased the power generated by the fuel cell by about 34%. The performance of the cell using 2 M acid gave comparable results to the 3 M acid. However, at higher current densities, the 3 M sulphuric acid resulted in the highest power density. The maximum power generated by the fuel cell using 3 M sulphuric acid was 31.6 mW cm^{-2} at a current density of 124 mA cm^{-2}, which improved the power density by approximately 8% when compared to 2 M sulphuric acid due to higher proton conductivity. A higher sulphuric acid concentration can, however, increase the adsorption of sulphate/bisulphate on the catalyst surface and degrade the catalyst faster [13]. Therefore, a 2 M sulphuric acid was chosen to conduct the rest of the experiments.

Table 4
Comparison of the performance of FE-DMFC for different MEAs.

Methanol concentration [M]	MEA type	Max power density [mW cm^{-2}]	Current density [mA cm^{-2}]
0.5	Type1	30.1	112.9
	Type2	34.6	132.4
	DMFC	42.7	129
2	Type1	33.7	136.3
	Type2	22	87.2
	DMFC	39.6	161.7

3.3. Effects of flowing electrolyte flow rate

The effect of the FE flow rate on the performance of the fuel cell has been shown in Fig. 9, where 2 M methanol and a 0.6 mm FE channel were used. Fig. 9 shows the polarisation curves with

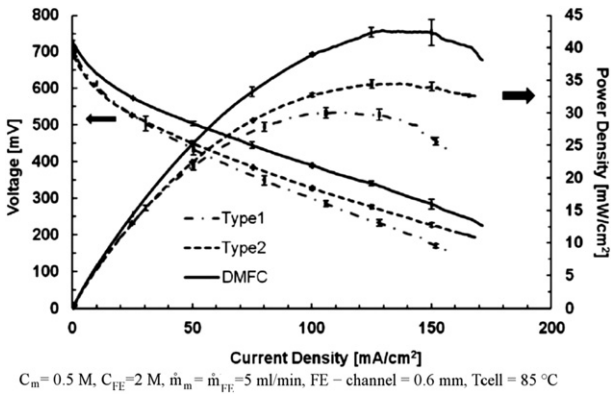

Fig. 6. Effects of MEA type on the performance using 0.5 M methanol.

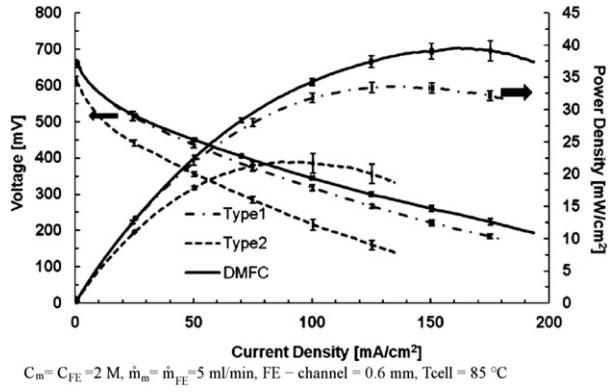

Fig. 7. Effects of MEA type on the performance using 2 M methanol.

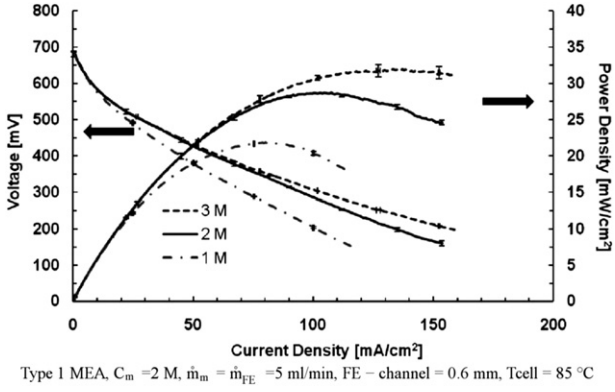

Fig. 8. Effects of FE concentration on performance.

respect to FE flow variations for 0, 3, 5, 8 and 10 ml min^{-1}. It can be seen from this figure that the open circuit voltage for no FE flow was about 600 mV, but the OCV increased to 650 and 700 mV for 3 and 5 ml min^{-1} of FE flow, respectively. The OCV changed minimally at higher flow rates. When no current was drawn from the cell (open circuit), reaction kinetic and methanol crossover losses were the only factors that contributed to the loss of voltage. Therefore, it can be concluded that the variations of the OCV when increasing of the FE flow rate is a result of the change in the amount of methanol crossover. This was also confirmed by looking at the power curves for different flow rates. Higher power densities have been achieved with higher flow rates. These results indicate that as FE flow rate increased, less methanol crossed over and higher power densities were obtained.

The maximum power density dependence on the FE flow rate was also studied for a 0.6 mm FE channel. Fig. 10 illustrates the results of this experiment and shows that the maximum power density increased when the flow rate was increased. For 2 M methanol, there is a 55% increase in the maximum power density after turning on the flowing electrolyte and adjusting the flow rate to 5 ml min^{-1}. However, there was minimal difference between the maximum power densities for 8, 10 and 13 ml min^{-1} flows,

Table 5
Effects of FE concentration on maximum power density.

Molarity [M]	Max power density [mW cm^{-2}]	Current density [mA cm^{-2}]
1	21.8	78.9
2	29.2	107.5
3	31.6	124.2

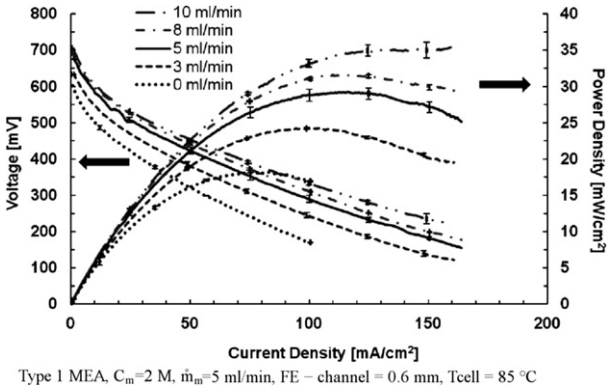

Fig. 9. Effects of FE flow rate.

especially for 0.5 M methanol. It can be concluded from these results that methanol crosses over to the cathode side where there is no FE flow and degrades the performance. However, as the FE flow rate increases, the amount of methanol that reaches the cathode decreases significantly. The asymptotic behaviour observed in this figure shows that the maximum power density reaches a stabilised point even though the flow rate increases, which indicates that the optimum flow rate has been reached.

3.4. Effects of flowing electrolyte channel thickness

Several flowing electrolyte channel thicknesses were tested. Fig. 11 shows the performance of the fuel cell for different FE channels operating under the same conditions (2 M methanol and 8 ml min^{-1} FE flow rate). These results demonstrate that the OCV of the thicker channels (1.5 and 2.0 mm) was approximately 700 mV whereas for the 0.6 mm channel, was 680 mV. This indicates that methanol crossover removal was more effective with thicker channels. Thicker channels, however, have more resistance due to longer electrode-to-electrode distance. By looking at the polarisation curves that are shown in Fig. 11, it can also be concluded that the 2.0 mm channel has a much higher slope than the two other channels, which is an indication of higher ohmic resistance. Therefore, the maximum power density generated by the 2 mm channel was about 11 mW cm^{-2} while 1.5 and 0.6 mm channels generate 30 and 31.6 mW cm^{-2}, respectively. The performance of the cell with the 1.5 mm channel was higher than the 0.6 mm channel for lower current densities, which indicated less methanol crossover. Finally, with increased current density, more methanol

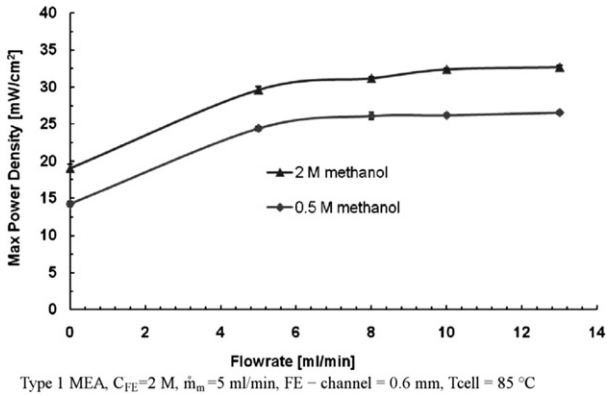

Fig. 10. Effects of FE flow rate on maximum power density.

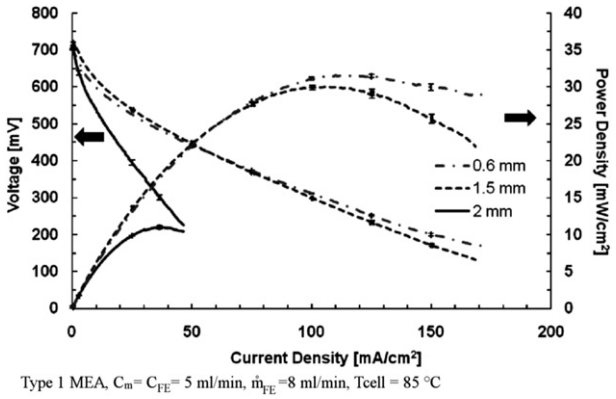

Fig. 11. Effects of FE thickness on performance.

was consumed on the anode side and less methanol was available to cross through the membrane. Therefore, an increase in the performance can be seen at higher current densities for the 0.6 mm channel, which is due to lower cell resistance as a result of lower electrode-to-electrode distance. Jayashree et al. also found that reducing the electrode-to-electrode distance resulted in an increase in the performance [12].

3.5. Effects of methanol concentration

The methanol concentration was one of the most important factors that affected the performance of the fuel cell. Fig. 12 shows the polarisation and power curves for 0.5, 2 and 4 M methanol for the 0.6 mm FE channel. By looking at the OCV in this figure, it can be concluded that a higher concentration of methanol results in lower OCV due to more methanol crossover (as discussed previously). As the current density was increased, the voltage that was produced by the 0.5 M methanol dropped faster, while 2 M methanol generated the highest power density of 34 mW cm^{-2}.

Table 4 shows that for a regular DMFC, the performance of fuel cell operating with 0.5 M methanol was higher. Other researchers have also reached the conclusion that 2 M methanol facilitated methanol crossover, which resulted in low performance. Therefore, it was evident that introducing the flowing electrolyte resulted in better performance of the fuel cell with a higher concentration of methanol, which was due to the removal of the crossed over methanol. A 4 M methanol test was also conducted. It is observed that the performance was lower than 0.5 M due to higher methanol

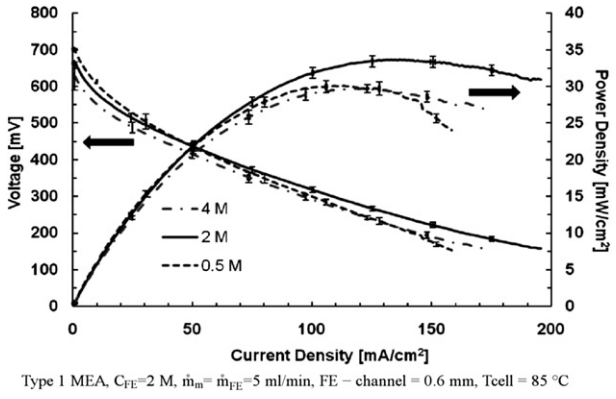

Fig. 12. Effects of methanol concentration on performance.

crossover. Although at very higher current densities, 0.5 M methanol showed mass transport limitations.

4. Conclusions

An experimental setup was designed, developed and operated. Also, a single cell FE-DMFC has been constructed and tested successfully. Several operating conditions such as the membrane thickness, sulphuric acid concentration, electrolyte flow rate, and flowing electrolyte channel thickness were tested. The performance of the fuel cell with respect to methanol concentration depended on the thickness of the Nafion® used in the MEA. For MEAs that use a thicker Nafion®, 2 M methanol with a 0.6 mm FE channel gave the maximum power density. For MEAs with a thinner membrane, 0.5 M methanol proved to be advantageous. It was concluded that although a thicker FE channel provides more adequate conditions for washing off the methanol, it also increased the internal resistance of the fuel cell. Therefore, a 0.6 mm channel was found to give the highest power density. The most advantageous electrolyte concentration was 2 M sulphuric acid. Also, it was found that increasing the flowing electrolyte flow rate improved the performance of the fuel cell. Although the FE-DMFC power results were lower when compared against a similar DMFC, it is conjectured here that further improvements and optimisations (channel geometry and component materials) in the current FE-DMFC design may lead to more competitive performance levels.

Acknowledgements

The authors would like to thank Ontario Centres of Excellence (OCE) and Natural Sciences and Engineering Research Council of Canada (NSERC) for their support.

References

[1] R. O'Hayre, S. Cha, W. Colella, Fuel Cell Fundamentals, John Wiley & Sons, Inc., 2006.
[2] N. DeLuca, Nafion blend membranes for the direct methanol fuel cell. PhD thesis, Drexel University, February 2008.
[3] R. Dillon, S. Srinivasan, A. Arico, V. Antonucci, in: N. Brandon, D. Thompsett (Eds.), Fuel Cells Compendium, Elsevier, 2005.
[4] V. Oliveira, C. Rangel, A. Pino, Int. J. Hydrogen Energy 34 (2009) 6443–6451.
[5] C. Spiegel, Designing and Building Fuel Cells, McGraw Hill, 2007.
[6] P. Kauranen, E. Skou, J. Appl. Electrochem. 26 (1996) 909–917.
[7] J. Villaluenga, B. Seoane, V. Barragn, C. Ruiz-Bauz, J. Colloid Interface Sci. 268 (2003) 476–481.
[8] T. Tschinder, T. Schaffer, S. Fraser, V. Hacker, J. Appl. Electrochem. 37 (2007) 711–716.
[9] J. Ling, O. Savadogo, J. Electrochem. Soc. 151 (2004) A1604–A1610.
[10] K. Kordesch, V. Hacker, U. Bachhiesl, J. Power Sourc. 96 (2001) 200–203.
[11] E. Kjeang, J. Goldak, M.R. Golriz, J. Gu, D. James, K. Kordesch, J. Power Sourc. 153 (2006) 90–99.
[12] R.S. Jayashree, S.K. Yoon, F.R. Brushett, P.O. Lopez-Montesinos, D. Natarajan, L.J. Markoski, P.J.A. Kenis, J. Power Sourc. 195 (2010) 3569–3578.
[13] R.S. Jayashree, M. Mitchell, D. Natarajan, L.J. Markoski, P.J.A. Kenis, Langmuir 23 (13) (2007) 6871–6874.
[14] E. Choban, J.S. Spendelow, L. Gancs, A. Wieckowski, P.J.A. Kenis, Electrochim. Acta 50 (2005) 5390–5398.
[15] A.S. Hollinger, R.J. Maloney, R.S. Jayashree, D. Natarajan, L.J. Markoski, P.J.A. Kenis, J. Power Sourc. 195 (2010) 3525–3528.
[16] K. Kordesch, Direct methanol fuel cell with circulating electrolyte, US Patent, 2003.
[17] A. Therdthianwong, P. Manomayidthikarn, S. Therdthianwong, Energy 32 (2007) 2401–2411.
[18] L. Tse, Membrane electrode assembly design for power design enhancement of direct methanol fuel cells. PhD thesis, Georgia Institute of Technology, Aug 2006.
[19] J. Zhang, G. Yin, Z. Wang, Q. Lai, K. Cai, J. Power Sourc. 165 (2007) 73–81.
[20] Y. Zhu, C. Liu, J. Liang, L. Wang, J. Power Sourc. 196 (2011) 264–269.
[21] V. Oliveira, C. Rangel, A. Pino, Chem. Eng. J. 157 (2010) 174–180.
[22] J. Koryta, J. Dvorak, L. Kavan, Principles of Electrochemistry, Wiley, 1993.
[23] M. Wright, An Introduction to Aqueous Electrolyte Solutions, Wiley, 2007.
[24] H. Darling, J. Chem. Eng. Data 9 (1964) 421–426.